THE JOURNAL OF PHYSICAL CHEMISTRY A LETTERS

2007, *111,* 415−418
Published on Web 12/30/2006

Driving Energies of Hydrogen Scrambling Motions in CH_5^+

Shan Xi Tian* and Jinlong Yang

Hefei National Laboratory for Physical Sciences at the Microscale and Department of Chemical Physics, University of Science and Technology of China, Hefei, Anhui 230026, China

Received: November 10, 2006; In Final Form: December 12, 2006

A comprehensive quantum chemistry study with natural bond orbital analysis is performed to reveal the intrinsic properties of the floppy potential energy surface of the smallest methonium ion CH_5^+. In contrast to the low-energy barriers of $\boldsymbol{C_s}$**(I)** → $\boldsymbol{C_s}$**(II)** → $\boldsymbol{C_s}$**(I)** and $\boldsymbol{C_s}$**(I)** → $\boldsymbol{C_{2v}}$ → $\boldsymbol{C_s}$**(I)** that correspond to the H_2 rotation and H-flip motions, the remarkably larger intramolecular interaction energies are the driving power to mimic the hydrogen scrambling in CH_5^+. As for the H_2 rotation and H-flip motions, the hyperconjugative and electrostatic interactions compete strongly. They together with other interactions compensate for each other and lead to the floppy potential energy surface.

The smallest protonated alkane, methonium ion CH_5^+, is a prototype of the intermediates in acid-catalyzed transformations of hydrocarbons and in the many electrophilic reactions,[1] and this novel cation receives much interest in interstellar chemistry.[2] However, debate stems from the floppiness of its potential energy surface (PES). Namely, five hydrogen atoms are scrambling freely and chemically equivalent in CH_5^+, or this cation prefers a quantum ground-state C_s symmetric structure having a three-center two-electron (3c−2e) bond.[3−11] Due to its highly fluxional structures predicted by the Monte Carlo[6] and quantum dynamics simulations,[5,12] CH_5^+ is known as chemistry's Cheshire Cat.[5] Some researchers believe that there is no final answer to CH_5^+ stability until the complex's Oka spectrum[13,14] can be assigned precisely.[15,16] Despite this controversy, the eclipsed C_s (noted as $\boldsymbol{C_s}$**(I)**), the staggered C_s (noted as $\boldsymbol{C_s}$**(II)**), and the C_{2v} symmetric conformers (shown in Figure 1) are statistically dominant in the dynamic simulations;[6,10,12] moreover, they are indeed the key to theoretically reproducing the infrared spectrum of CH_5^+.[15,16]

High-level ab initio quantum chemistry studies indicate that the $\boldsymbol{C_s}$**(II)** and $\boldsymbol{C_{2v}}$ conformers correspond to two low-lying saddle points connecting the isomerization motions shown in Figure 1. The energy barriers are 0.1[7] or 0.083[9] kcal/mol and 0.8[7] or 0.974[9] kcal/mol for the H_2 rotation (via $\boldsymbol{C_s}$**(II)**) and H-flip (via $\boldsymbol{C_{2v}}$), respectively. These two paths correspond to the most important motions of hydrogen scrambling on the floppy PES. They together with various quantum effects (e.g., vibrational coupling, nuclear spin statistics, and tunneling splits) lead to the complexity of the rovibrational spectrum, in particular, in the low-frequency region.[15,16] In this letter, natural bond orbital (NBO)[17] analyses based on second-order Møller−Plesset perturbation (MP2) calculations are performed. We focus on the electronic properties of CH_5^+ and the roles of the different intramolecular interactions in constructing the floppy PES, in particular, the driving energies of the H_2 rotation and H-flip motions. The amplitudes and correlations of these energetic contributions are the key to revealing why and how this Cheshire Cat is smiling, namely, toward an understanding of the structural stability of CH_5^+ and the floppiness of its PES.

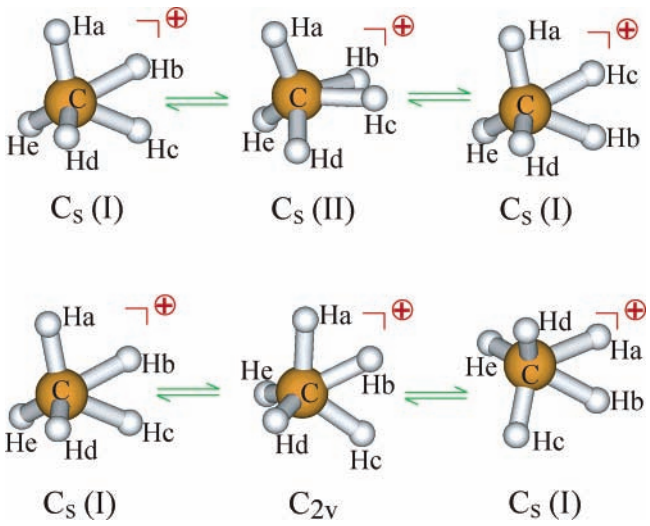

Figure 1. H_2 rotation between the global minimum $\boldsymbol{C_s}$**(I)** and the transition conformer $\boldsymbol{C_s}$**(II)** (top panel). H-flip between the global minimum $\boldsymbol{C_s}$**(I)** and the transition conformer $\boldsymbol{C_{2v}}$ (bottom panel).

The reliability of the NBO theorem to analyze the structural stability has been demonstrated by an excellent work on the internal rotation of ethane.[18] Recently, the NBO theorem was also successfully applied in a study of intramolecular hydrogen bonding.[19] In the NBO theorem, three principle physical factors, Pauli exchange (E_x), electrostatic (E_s), and hyperconjugative interaction (E_h), determine the molecular structural preference.[20] The steric E_x value arises from wave function antisymmetry; E_s includes nuclear−nuclear, electron−electron, and nuclear−electron Coulombic interactions; E_h represents charge transfer between two localized orbitals, the occupied bonding orbital σ_i and the unoccupied antibonding orbital σ_j*. In the NBO

* Author to whom correspondence should be addressed. E-mail: sxtian@ustc.edu.cn.

10.1021/jp067450j CCC: $37.00

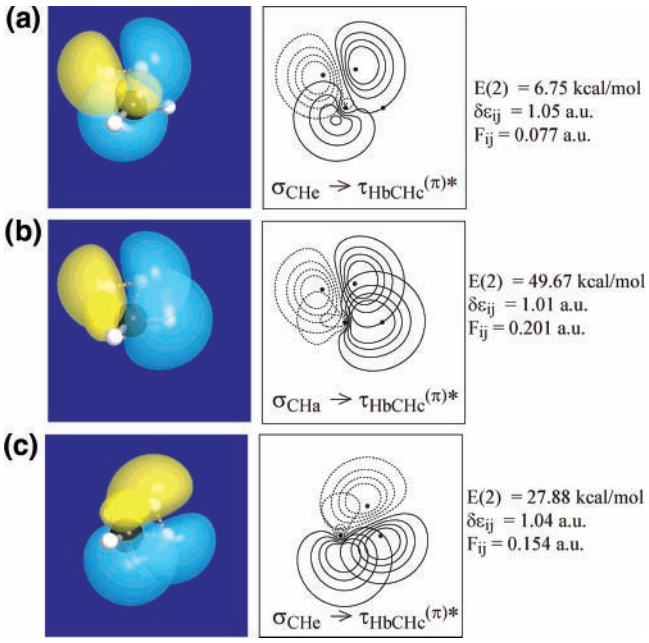

Figure 2. Predominating hyperconjugative interactions in (a and b) C_s**(I)** and (c) C_s**(II)**. Three-dimensional (left) and two-dimensional contour maps (middle) and the second-order perturbation energies (right) are presented.

analyses, the total E_h values were calculated by summation of the second-order perturbation energies $E(2)$ of the vicinal and geminal charge transfers, $E(2) = -q_i F_{ij}^2/\delta\epsilon_{ij}$, where q_i was the donor orbital occupancy, $\delta\epsilon_{ij}$ was the orbital energy difference, and F_{ij} was the off-diagonal NBO Fock matrix element.[17] The geometrical parameters of the C_s**(I)**, C_s**(II)**, and C_{2v} conformers were fully optimized at the MP2/aug-cc-pVTZ level, and the stabilities on the PES were examined by harmonic vibrational frequency calculations. The global minimum conformer C_s**(I)** and the first-order saddle points C_s**(II)** and C_{2v} were rationalized at the MP2/aug-cc-pVTZ level, and the C_s**(II)** and C_{2v} conformers were further characterized by the intrinsic reaction coordinate (IRC) calculations. To obtain the IRC energies, the geometries were optimized at each point along the IRC path pointing to the stable C_s**(I)** conformer. All energetic calculations and NBO analyses were carried out with the Gaussian 03[21] and NBO 5.0[22] programs.

According to NBO theorem, the energy barrier of the H_2 rotation or the H-flip transition is $\Delta E_{HF} = \Delta E_x + \Delta E_s + \Delta E_h$ in the Hartree−Fock (HF) approximation.[20] Since the electron correlation effect is included in the MP2 calculations, the real energy barrier predicted at the MP2 level $\Delta E = \Delta E_{HF} + \Delta E_c$, where ΔE_c represents the electron correlation effect. Two isomerization paths show that the energy barriers ΔE are 0.144 and 0.558 kcal/mol^{-1} for C_s**(I)** → C_s**(II)** → C_s**(I)** (H_2 rotation) and C_s**(I)** → C_{2v} → C_s**(I)** (H-flip), respectively. The reliability of the present calculations is proven by a comparison with the results obtained at the higher-level ab initio calculations.[7,9]

It is well-known that there is a distinct 3c−2e bond τ_{HCH} in C_s**(I)** and C_s**(II)** (Figure 1S of the Supporting Information). As shown in Figure 2, delocalization processes arise from the predominant hyperconjugative interactions of $\sigma_{CHd(e)} \rightarrow \tau_{HbCHc}^{(\pi)*}$ and $\sigma_{CHa} \rightarrow \tau_{HbCHc}^{(\pi)*}$ for C_s**(I)** and $\sigma_{CHd(e)} \rightarrow \tau_{HbCHc}^{(\pi)*}$ for C_s**(II)**. Here $\sigma_{CHd(e)}$ and $\tau_{HbCHc}^{(\pi)*}$ represent the occupied C−H bond and the 3c−2e antibond, respectively. The total E_h of each stationary conformer is obtained by summation of all vicinal and geminal hyperconjugation energies. The extremely strong hyperconjugative interactions among C, Ha, Hb, and Hc in the C_{2v} conformer indicate the possibility of a four-center four-electron hyperbond.[11] By extracting a C−H bond energy[23] from the total E_h of the C_{2v} conformer, its E_h, E_x, E_c, and ΔE_s values can be determined; these quantities for the C_{2v} conformer as well as the values of the other two conformers are listed in Table 1. One can find that the vicinal hyperconjugative interaction plays a role in the total E_h. The higher E_h implies more stabilization.[17−20] The typical negative exchange energies for the valence natural localized molecular orbitals C−H lead to the negative total E_x values. The above two types of interactions are competitive in C_s**(I)** and C_s**(II)**, while E_x is much smaller than E_h for C_{2v}. The ΔE_s is a large negative value, leading to less stability of C_{2v}. It also deserves attention that the electron correlation effect (128−130 kcal/mol) is important to predict accurate energy differences for these species.

TABLE 1: Energetic Compositions (in kcal/mol) of Intramolecular Interactions in the Stationary Structures.

	C_s**(I)**	C_s**(II)**	C_{2v}
E_h	77.38	66.29	163.26 [b]
vicinal part	65.17	56.80	153.10 [b]
geminal part	12.21	9.49	10.16
E_x	−70.65	−68.19	−68.70
ΔE_s [a]	0.00	8.55	−94.59 [b]
E_c [c]	128.51	128.73	130.28

[a] The relative energies are given with respect to C_s**(I)** species. [b] This value excludes bond energy C−Hb (329.78 kcal/mol from ref 23). [c] E_c is estimated by E(MP2) − E(HF).

The various interaction energies are given in the Table 1S of the Supporting Information. To our surprise, these energy values are much larger than the energy barriers ΔE of C_s**(I)** → C_s**(II)** → C_s**(I)** (H_2 rotation) and C_s**(I)** → C_{2v} → C_s**(I)** (H-flip). It suggests that these different interaction energies should lead to an activation of five hydrogen atoms and yield the freely scrambling motions in CH_5^+. Furthermore, the nuclear skeleton motion (i.e., vibrational) energies are normally much smaller than these interaction energies, implying that the hydrogen scrambling is most likely due to the electronic properties of CH_5^+. The relative energies are calculated with respect to the C_s**(I)** values, and they are plotted in terms of the IRC paths in Figure 3. In general, the ΔE values are predominantly determined by ΔE_x, ΔE_s, and ΔE_h. In part a, ΔE_h decreases along the IRC path of C_s**(I)** → C_s**(II)**, while ΔE_s and ΔE_x increase. This implies that the H_2 rotation to C_s**(I)** is controlled by the hyperconjugative interactions. Namely, the hyperconjugative interactions, mostly of $\sigma_{CHd(e)} \rightarrow \tau_{HbCHc}^{(\pi)*}$ and $\sigma_{CHa} \rightarrow \tau_{HbCHc}^{(\pi)*}$, play an essential role in the stabilization of the eclipsed conformer C_s**(I)**. However, there may be some local minima around staggered C_s**(II)** on the PES without the hyperconjugative interactions, because E_x and E_s values are typically negative, which yields the antibarrier for the H_2 rotation transition C_s**(I)** → C_s**(II)** → C_s**(I)**. In contrast to the H-flip process, ΔE_s decreases dramatically along the C_s**(I)** → C_{2v} path shown in part b. The electrostatic interaction as well as the Pauli exchange interaction play a role in stabilizing C_s**(I)** during the H-flip. In general, the hyperconjugative and electrostatic interactions compensate for each other, resulting in the low-energy barrier. Moreover, the electron correlation effects on the barrier are shown in Figure 2S of the Supporting Information. There the more floppy PES shows more than one local minima for the H_2 rotation process if the electron correlation (E_c) is excluded or considered insufficiently. However, the electron correlation lowers the barrier of the H-flip process.

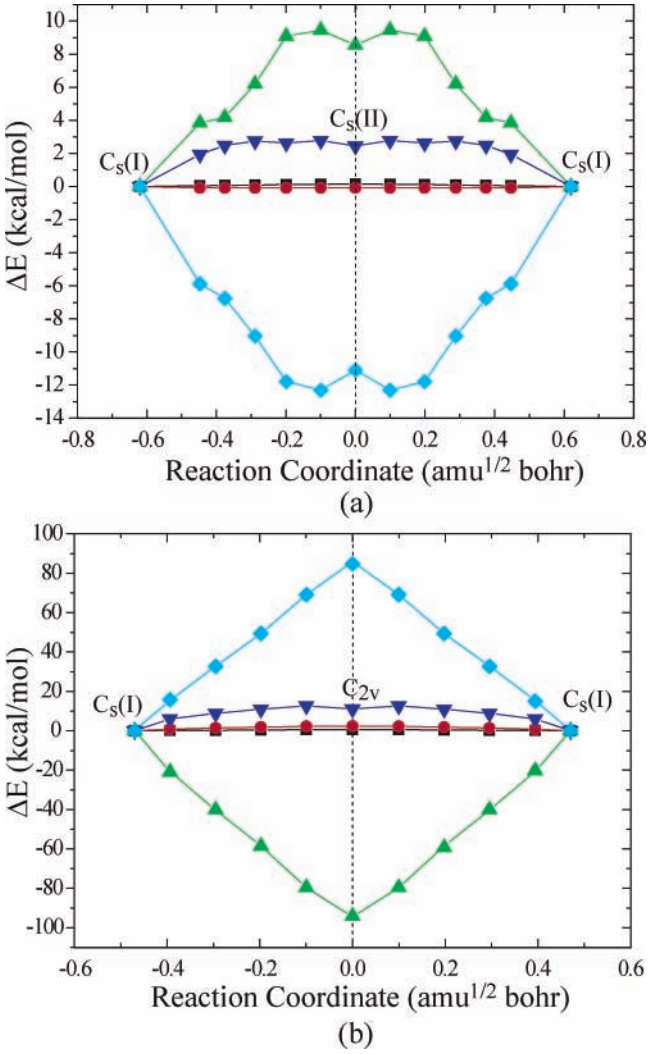

Figure 3. Energy dependencies of the IRC paths: (a) H_2 rotation and (b) H-flip. The energies of ΔE (■, black), ΔE_{HF} (●, red), ΔE_s (▲, green), ΔE_x (▼, blue), and ΔE_h (◆, cyan) are calibrated, respectively, by the values of C_s**(I)**.

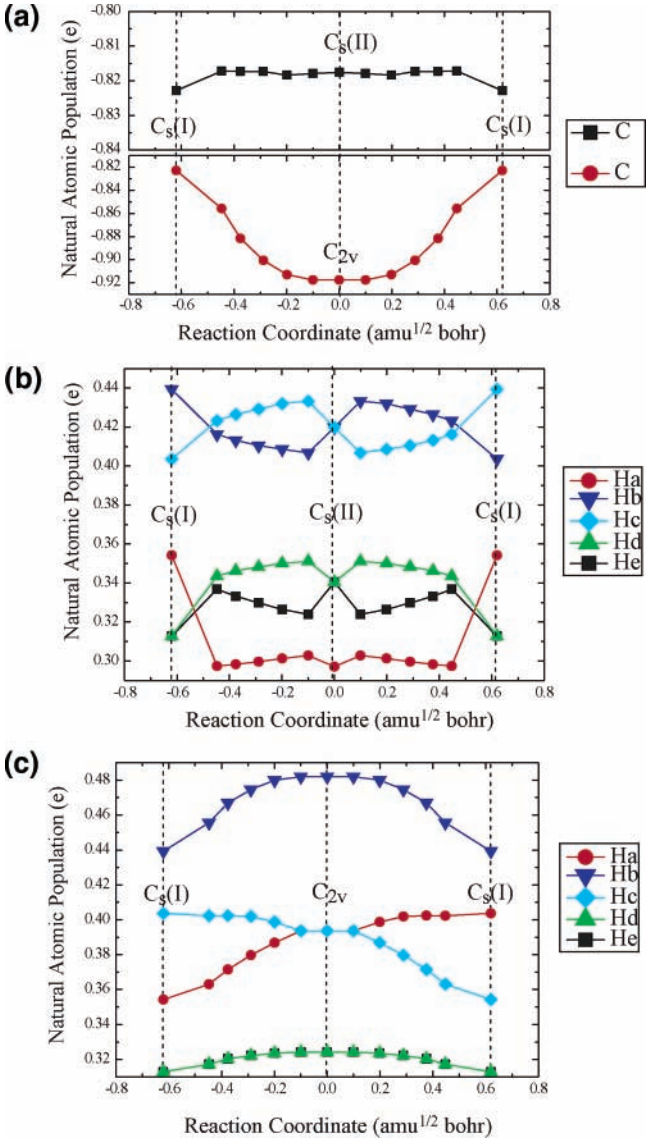

Figure 4. Natural atomic population change for each atom in C_s**(I)** → C_s**(II)** → C_s**(I)** and C_s**(I)** → C_{2v} → C_s**(I)**.

The natural atomic populations (NAPs) based on the NBO analyses are shown in Figure 4. In part a, the negative NAP value of the carbon atom decreases slightly along C_s**(I)** → C_s**(II)** (H_2 rotation), while it increases with a large margin along C_s**(I)** → C_{2v} (H-flip). As shown in parts b and c, the H_2 rotation in the C_s**(I)** → C_s**(II)** → C_s**(I)** process leads to an alternation of the NAPs of Hb and Hc, while H-flip in the C_s**(I)** → C_{2v} → C_s**(I)** process results in an alternation of Ha and Hc. In general, the Columbic interactions between carbon and hydrogen atoms vary more drastically from C_s**(I)** to C_{2v} than those from C_s**(I)** to C_s**(II)**. This is in line with the scenario that there are more significant ΔE_s variances shown in Figure 3b.

The comprehensive analyses of the intramolecular interactions and their contributions to the floppy PES of CH_5^+ mimic the proton scrambling that is proposed by the dynamic simulations. In contrast to the low-energy barriers of C_s**(I)** → C_s**(II)** → C_s**(I)** and C_s**(I)** → C_{2v} → C_s**(I)**, which correspond to the H_2 rotation and H-flip motions, the remarkably larger intramolecular interaction energies are the key to stimulating the hydrogen scrambling, i.e., the Cheshire Cat's smiling. As for the H_2 rotation and H-flip motions, the hyperconjugative and electrostatic interactions compete strongly. They together with other interactions compensate for each other and lead to the floppy PES. The methods used in this work are promisingly feasible to reveal the tautomerism or isomerism, namely, the driving forces of atoms to form the stable molecular structures.

Acknowledgment. This work is partially supported by the National Natural Science Foundation of China (Grant Nos. 20503026, 20673105, 20533030, and 50121202) and the Scientific Research Foundation for Returned Overseas Chinese Scholars, State Education Ministry.

Supporting Information Available: The occupied and unoccupied 3c−2e hyperbonds, energy changes along the IRCs, and the electron correlation effects along the IRCs. This material is available free of charge via the Internet at http:// pubs.acs.org.

References and Notes

(1) Olah, G. A.; Klopman, R.; Schlosberg, R. H. *J. Am. Chem. Soc.* **1969**, *91*, 3261.
(2) Herbst, E. *J. Phys. Chem. A* **2005**, *109*, 4017.
(3) Schreiner, P. R. *Angew. Chem., Int. Ed.* **2000**, *39*, 3239.
(4) Olah, G. A.; Rasul, G. *Acc. Chem. Res.* **1997**, *30*, 245.
(5) Marx, D.; Parrinello, M. *Science* **1999**, *284*, 59.
(6) Thompson, K. C.; Crittenden, D. L.; Jordan, J. T. *J. Am. Chem. Soc.* **2005**, *127*, 4954.

(7) Schreiner, P. R.; Kim, S.-J.; Schaefer, H. F., III.; Schleyer, P. v. R. *J. Chem. Phys.* **1993**, *99*, 3716.

(8) Müller, H.; Kutzelnigg, W.; Noga, J.; Klooper, W. *J. Chem. Phys.* **1997**, *106*, 1863.

(9) Jin, Z.; Braams, B. J.; Bowman, J. M. *J. Phys. Chem. A* **2006**, *110*, 1569.

(10) Marx, D.; Savin, A. *Angew. Chem., Int. Ed. Engl.* **1997**, *36*, 2077.

(11) Okulik, N. B.; Peruchena, N. M.; Jubert, A. H. *J. Phys. Chem. A* **2006**, *110*, 9974.

(12) Marx, D.; Parrinello, M. *Nature* **1995**, *375*, 216.

(13) White, E. T.; Tang, J.; Oka, T. *Science* **1999**, *284*, 135.

(14) See arguments in: Kramer, G. M.; Oka, T.; White, E. T.; Marx, D.; Parrinello, M. *Science* **1999**, *286*, 1051

(15) Asvany, O.; Kumar, P. P.; Redlich, B.; Hegemann, I.; Schlemmer, S.; Marx, D. *Science* **2005**, *309*, 1219.

(16) Huang, X.; McCoy, A. B.; Bowman, J. M.; Johnson, L. M.; Savage, C.; Dong, F.; Nesbitt, D. J. *Science* **2006**, *311*, 60.

(17) Weinhold, F.; Landis, C. R. *Valency and Bonding*; Cambridge University Press: Cambridge, U. K., 2005.

(18) Pophristic, V.; Goodman, L. *Nature* **2001**, *411*, 565.

(19) Tian, S. X.; Yang, J. *Angew. Chem., Int. Ed.* **2006**, *45*, 2069.

(20) Goodman, L.; Gu, H.; Pophristic, V. *J. Chem. Phys.* **1999**, *110*, 4268.

(21) Frisch, M. J.; Trucks, G. W.; Schlegel, H. B.; Scuseria, G. E.; Robb, M. A.; Cheeseman, J. R.; Montgomery, J. A., Jr.; Vreven, T.; Kudin, K. N.; Burant, J. C.; Millam, J. M.; Iyengar, S. S.; Tomasi, J.; Barone, V.; Mennucci, B.; Cossi, M.; Scalmani, G.; Rega, N.; Petersson, G. A.; Nakatsuji, H.; Hada, M.; Ehara, M.; Toyota, K.; Fukuda, R.; Hasegawa, J.; Ishida, M.; Nakajima, T.; Honda, Y.; Kitao, O.; Nakai, H.; Klene, M.; Li, X.; Knox, J. E.; Hratchian, H. P.; Cross, J. B.; Bakken, V.; Adamo, C.; Jaramillo, J.; Gomperts, R.; Stratmann, R. E.; Yazyev, O.; Austin, A. J.; Cammi, R.; Pomelli, C.; Ochterski, J. W.; Ayala, P. Y.; Morokuma, K.; Voth, G. A.; Salvador, P.; Dannenberg, J. J.; Zakrzewski, V. G.; Dapprich, S.; Daniels, A. D.; Strain, M. C.; Farkas, O.; Malick, D. K.; Rabuck, A. D.; Raghavachari, K.; Foresman, J. B.; Ortiz, J. V.; Cui, Q.; Baboul, A. G.; Clifford, S.; Cioslowski, J.; Stefanov, B. B.; Liu, G.; Liashenko, A.; Piskorz, P.; Komaromi, I.; Martin, R. L.; Fox, D. J.; Keith, T.; Al-Laham, M. A.; Peng, C. Y.; Nanayakkara, A.; Challacombe, M.; Gill, P. M. W.; Johnson, B.; Chen, W.; Wong, M. W.; Gonzalez, C.; Pople, J. A. *Gaussian 03*, revision C.02; Gaussian, Inc.: Wallingford, CT, 2004.

(22) Glendening, E. D.; Badenhoop, J. K.; Reed, A. E.; Carpenter, J. E.; Bohmann, J. A.; Morales, C. M.; Weinhold, F. *NBO*, version 5.0; Theoretical Chemistry Institute, University of Wisconsin at Madison: Madison, WI, 2001.

(23) Stockbauer, R. *Int. J. Mass Spectrom. Ion Phys.* **1977**, *25*, 89.